Measurement of the Field-Free Alignment of Diatomic Molecules

Nan Xu, Chengyin Wu,* Yunan Gao, Hongbing Jiang, Hong Yang, and Qihuang Gong*

State Key Laboratory for Mesoscopic Physics and Department of Physics, Peking University, Beijing 100871, People's Republic of China

Received: July 20, 2007; In Final Form: October 18, 2007

An apparatus was constructed to experimentally quantify the field-free alignment of diatomic molecules irradiated by strong femtosecond laser pulses. In this apparatus, both homodyne and pure heterodyne detections were realized. The alignment signal is proportional to $[\langle\cos^2\theta\rangle - 1/3]^2$ for homodyne detection and $(\langle\cos^2\theta\rangle - 1/3)$ for pure heterodyne detection, where θ is the polar angle between the molecular axis and the laser polarization direction. Fourier transform spectra of the homodyne signal and the pure heterodyne signal were also studied. By comparing the alignment signal and its Fourier transform spectrum with the numerical calculation of the time-dependent Schrödinger equation, we demonstrated that the pure heterodyne signal directly reproduced the alignment parameter $\langle\cos^2\theta\rangle$, and its Fourier transform spectrum provided information regarding the populations of different J states in the rotational wavepacket.

Introduction

Intense laser pulses can align molecules due to the interaction between the laser electric field and the induced dipole moment of molecules. If the laser pulse duration is longer than the rotational period of the molecule, each eigenstate of the field-free rotational Hamiltonian evolves adiabatically into the corresponding eigenstate of the instantaneous Hamiltonian and returns to its original state after the laser pulse. This alignment is called adiabatic alignment.[1−3] If the laser pulse duration is shorter than the rotational period of the molecule, the laser−molecule interaction gives the molecule a rapid "kick" to move the molecular axis toward the laser field direction. After the laser pulse, the transient alignment can periodically be revived as long as the coherence of the rotational wavepacket is preserved. This alignment is called field-free alignment.[4−6] In comparison with adiabatic alignment, field-free alignment has the obvious advantage of not interfering with subsequent applications. Therefore, field-free-aligned molecules have been widely applied in the past few years. For example, by measuring the ion yield or the high harmonic intensity from the aligned nitrogen molecule in intense femtosecond laser fields, Litvinyuk et al.[7] directly obtained its angle-dependent ionization rate, and Itatani et al.[8] accomplished a tomographic reconstruction of its highest-occupied molecular orbital. Recently, Kanai et al. reported that aligned molecules could serve as an ideal quantum system to investigate the quantum phenomena associated with molecular symmetries.[9]

The alignment degree of molecules is characterized by the average of $\langle\cos^2\theta\rangle$, where θ is the angle between the laser polarization direction and the molecular axis. The $\langle\cos^2\theta\rangle = 1/3$ represents an isotropic angular distribution evenly distributed across all θ. If $\langle\cos^2\theta\rangle > 1/3$, the molecule is predominantly aligned along the laser polarization direction. If $\langle\cos^2\theta\rangle < 1/3$, the probability distribution for the axis of the molecule is concentrated around a plane orthogonal to the laser polarization direction and labeled as an antialignment. There are two typical experimental methods to evaluate the alignment degree of molecules. One is Coulomb explosion and dissociative ionization, in which the aligned molecules are quickly broken by another strong probe laser pulse.[10,11] The angular distributions of the fragmental ions directly represents the alignment degree of the molecules. The disadvantage of this method is that the strong probe laser pulse destroys the aligned molecules and induces additional alignment. The other method to evaluate the alignment degree of molecules is the weak-field polarization technique, in which another weak probe laser pulse is used to measure the birefringence induced by the transient aligned molecules. The depolarization of the probe laser represents the alignment degree of the molecules.[12−14] This method has the advantage that the weak probe laser does not affect the aligned molecules. The weak field polarization technique has homodyne and heterodyne detection modes.[12,13] The alignment signal is proportional to $[\langle\cos^2\theta\rangle - 1/3]^2$ for homodyne detection and $(\langle\cos^2\theta\rangle - 1/3)$ for pure heterodyne detection. Compared with the homodyne signal, the pure heterodyne signal had the merit of directly reproducing the alignment parameter $\langle\cos^2\theta\rangle$, except with a 1/3 baseline shift. Unfortunately, the pure heterodyne signal is hardly obtained in the experimental

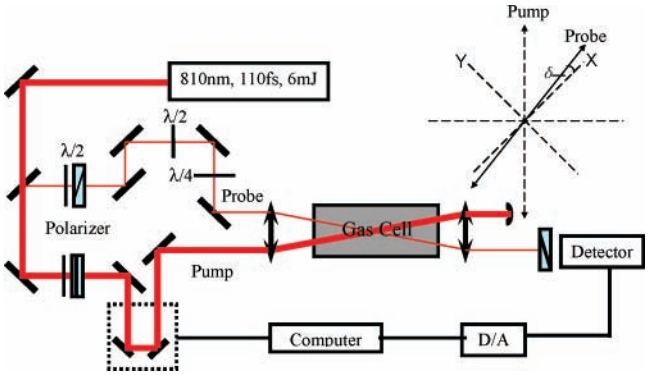

Figure 1. Experimental setup for measuring the field-free alignment of molecules induced by strong femtosecond laser pulses. The optic axis of the quarter waveplate was along the *X* direction, 45° with respect to the pump laser polarization. The signal electric field in the *Y* direction was collected by a detector.

* To whom correspondence should be addressed. E-mail: cywu@pku.edu.cn (C.W.); qhgong@pku.edu.cn (Q.G.).

10.1021/jp075728h CCC: $40.75 © 2008 American Chemical Society
Published on Web 01/09/2008

measurement; homodyne detection is still commonly used, until now. However, the homodyne signal does not indicate whether the aligned molecule is parallel or perpendicular to the laser polarization direction.

In this article, we modified the typical weak-field polarization technique. Both homodyne and pure heterodyne detection were realized in this experimental apparatus. They were employed to quantify the post-pulse alignment of the diatomic molecules irradiated by a strong femtosecond laser pulse. The alignment signal and its Fourier transform spectrum were analyzed and compared with the numerical calculation of the time-dependent Schrödinger equation.

Experimental Setup

The experiment setup is shown in Figure 1, which was a modification of a typical weak-field polarization technique described elsewhere.[15] An 800 nm, 110 fs laser pulse was divided into two parts to provide a strong energy pump beam and a weak energy probe beam, both linearly polarized at 45° with respect to each other. An optical translational stage controlled by a stepping motor was placed on the pump beam path in order to precisely adjust the relative separation times between the two pulses. Both the pump beam and the probe beam were focused with a 30 cm focal length lens into a 20 cm long gas cell at a small angle. The gas cell was filled with different gases at room temperature under one atmospheric pressure. The field-free-aligned molecules induced by the strong pump laser caused birefringence and depolarized the probe laser. The depolarization of the probe laser, which represents the alignment degree, was analyzed with a polarizer set at 90° with respect to its initial polarization direction. The alignment signals were detected by a photoelectric cell and transformed into a computer via a four-channel A/D converter for analysis.

The main modification was that a $\lambda/4$ waveplate was inserted in the probe laser path before the gas cell. Figure 1 also shows the relative directions of the laser polarizations, the optic axis of the quarter waveplate, and the signal field. The optic axis of the quarter waveplate was along the *X* direction, 45° with respect to the pump laser polarization. The signal electric field in the *Y* direction was collected by a detector. When the probe laser polarization was along the optic axis of the quarter waveplate, this was the commonly used homodyne detection. When the probe laser polarization was a little off from the optic axis of the quarter waveplate ($\delta < 5°$), the linearly polarized probe laser became elliptical after the quarter waveplate. In addition to the transient birefringence caused by the aligned molecules, the *Y* component of the laser electric field was also collected by the detector. The detection became heterodyne. The pure heterodyne alignment signal was obtained by subtracting the two heterodyne signals measured, respectively, by a left-handed and right-handed elliptically polarized probe laser.

Theory

1. Rotational Wavepacket Revival. A diatomic molecule illuminated by a linearly polarized laser pulse is a model of a rigid rotor interacting with the electric field through the induced dipole moment. The time evolution of the laser−molecule system is described by the time-dependent Schrödinger equation

$$i\hbar \frac{\partial \Psi(t)}{\partial t} = H\Psi(t) \tag{1}$$

and the instantaneous Hamiltonian can be written as[1]

$$H = BJ^2 - U_0(t)\cos^2\theta \tag{2}$$

where BJ^2 is the rotational energy operator, θ is the angle between the molecular axis and the laser polarization direction, and

$$U_0(t) = \frac{1}{4}(\alpha_{||} - \alpha_{\perp})\epsilon^2(t) \tag{3}$$

where $\alpha_{||}$ and $\alpha_{\perp}$ are the components of the polarizability parallel and perpendicular to the molecular axis, respectively. The $\epsilon(t)$ denotes the laser field distribution with the time.

The time-dependent wave function is expanded as

$$|\Psi(t)\rangle = \sum_{J,M} A_{J,M}(t)|J,M\rangle \tag{4}$$

where $A_{J,M}(t)$ is the time-dependent expanding coefficient and $|J,M\rangle$ are spherical harmonics. At the end of the laser−molecule interaction, the expanding coefficient $A_{J,M}$ can be numerically calculated using the Cranck−Nicholson method.[16] After the laser pulse, the wavepacket evolves as

$$|\Phi(t)\rangle = \sum_{J,M} A_{J,M}(t)e^{-iE_J t}|J,M\rangle \tag{5}$$

where E_J is the rotational energy eigenvalue given by $E_J = BJ(J+1)$. This equation indicates that after a molecular rotational period, the wavepacket will exactly reproduce the initial state of the field-free evolution. Such behavior is called a wavepacket revival.

The quantity characterizing the alignment can be numerically calculated. Note that all transitions occur between J and $J \pm 2$ because only the matrix elements $\langle J,M|\cos^2\theta|J,M\rangle$ and $\langle J,M|\cos^2\theta|J \pm 2,M\rangle$ are not equal to zero according to the properties of spherical harmonic functions; thus, the average value of $\langle\cos^2\theta\rangle$ is given by[11]

$$\langle\cos^2\theta\rangle(t) = \langle\Phi(t)|\cos^2\theta|\Phi(t)\rangle = \sum_{J,M}[|A_{J,M}|^2 C_{J,J,M} + 2|A_{J,M}||A_{J+2,M}|C_{J,J+2,M}\cos(\Delta\omega_J t + \varphi_{J,J+2})] \tag{6}$$

where $\Delta\omega_J = (E_{J+2} - E_J)/\hbar$ is the Raman frequency, $C_{J,J+2,M}$ is the coupling of $|J,M\rangle$ to $|J+2,M\rangle$, and $\varphi_{J,J+2}$ denotes the relative phase between the states $|J,M\rangle$ and $|J+2,M\rangle$ at the end of the pump laser. It should be mentioned that $\varphi_{J,J+2}$ depends on the rotational quantum number J.

Given a macroscopic system with a rotational temperature T, we calculate the rotational wavepacket dynamics $\langle\cos^2\theta\rangle(t)_{J,M}$ for each initial rotational state $|J,M\rangle$. The alignment parameter is obtained by averaging the $\langle\cos^2\theta\rangle(t)_{J,M}$ over all initial rotational states $|J,M\rangle$ weighted by the Boltzmann distribution

$$\langle\cos^2\theta\rangle(t) = \frac{\sum_{J,M} g_J \exp(-E_J/kT)\langle\cos^2\theta\rangle(t)_{J,M}}{\sum_J g_J(2J+1)\exp(-E_J/kT)} \tag{7}$$

and g_J is the nuclear spin statistics factor of a homonuclear diatomic molecule.

2. Measurement of Field-Free Molecular Alignment. The state vector of the free molecule denoted by $\Phi(t)$ was probed by a nonresonant weak laser pulse. When the probe laser polarization was a little off from the optic axis of the quarter waveplate, the linearly polarized probe laser became slightly elliptical after the quarter waveplate. Supposing that δ is the angle between the probe laser polarization and the optic axis of the quarter waveplate, the probe electric field after the quarter waveplate is written as

$$\vec{E}_{\text{probe}}(\tau) = \vec{e}_X E_X \exp[-i\omega(t-\tau)] + \vec{e}_Y E_Y \exp[-i\omega(t-\tau) + i\pi/2] \quad (8)$$

where τ is the time delay between the pump and the probe laser pulses. The ellipticity $\epsilon = |E_Y/E_X| = |\tan\delta|$ determines the relative magnitudes of the electric field components in the Y and X directions. It should be noticed that there is a $\pi/2$ phase shift between E_X and E_Y.

When the pump laser did not fire, E_X was blocked by the polarizer before the detector, and only E_Y was collected by the detector. When the pump laser did fire, the molecules were aligned and caused a transient birefringence. When the probe laser traveled through the aligned molecules, E_X was depolarized and produced a signal electric field $E_s(\tau)$ in the Y direction. With the approximations of a slowly varying envelope and the small amplitude of the signal wave, the signal electric field $E_s(\tau)$ was determined by[12,17]

$$E_s(\tau) = \frac{3\pi l\omega\Delta\alpha N}{4nc}\left(<\cos^2\theta>_\tau - \frac{1}{3}\right)E_X \exp(-i\omega(t-\tau) + i\pi/2) \quad (9)$$

where l is the distance that the probe laser traveled in the aligned molecules, $\Delta\alpha = \alpha_{||} - \alpha_\perp$ is the anisotropy of the molecular dynamical polarizability, N is the molecular number density, n is the average value of the molecular refractive index, and c is the speed of the light. It should be mentioned that there was also a $\pi/2$ phase shift between the signal field $E_s(\tau)$ and the probe laser electric field E_X.

In the same way, E_Y was also depolarized after traveling through the aligned molecules. However, compared with E_Y itself, the variation of E_Y in the Y direction can be neglected. Therefore, the signal intensity collected by the detector can be written as

$$I_{\text{sig}}(\tau) = \eta \int_{\tau-T_d/2}^{\tau+T_d/2} |E_s(t) + E_Y \exp[-i\omega(t-\tau) + i\pi/2]|^2 dt \propto \left[\left(<\cos^2\theta>_\tau - \frac{1}{3}\right) + C\right]^2 \quad (10)$$

where T_d is the response time of the detector, which is much longer than the pulse width of the probe laser, and η is the detection efficiency. The parameter $C = 4nc\tan\delta/(3\pi l\omega\Delta\alpha N)$ denotes the constant contribution from the Y electric field component of the slightly elliptically polarized laser. Its magnitude and sign were determined, respectively, by the ellipticity and the rotation direction of the elliptical polarized probe laser after the quarter waveplate.

When the probe laser polarization was along the optic axis of the quarter waveplate (i.e., $\delta = 0$), the parameter C representing the external electric field contribution equaled zero. This was the commonly used homodyne detection, and the alignment signal was proportional to $[<\cos^2\theta> - 1/3]^2$. When the probe laser polarization was a little off from the optic axis of the quarter waveplate ($\delta < 5°$), the linearly polarized probe laser became slightly elliptical after the quarter waveplate, and the detection became heterodyne. The alignment signal is proportional to $[<\cos^2\theta> - 1/3 + C]^2$. The pure heterodyne signals are derived from the difference between the two heterodyne signals with opposite parameter C

$$I_{\text{pure signal}}(\tau) = I_{\text{sig}}^{\text{positive}}(\tau) - I_{\text{sig}}^{\text{negative}}(\tau) \propto \left\{\left[\left(<\cos^2\theta>_\tau - \frac{1}{3}\right) + |C|\right]^2 - \left[\left(<\cos^2\theta>_\tau - \frac{1}{3}\right) - |C|\right]^2\right\} = 4|C|\left(<\cos^2\theta>_\tau - \frac{1}{3}\right) \quad (11)$$

The opposite parameter C was realized by tilting the probe laser polarization to opposite directions relative to the optic axis of the quarter waveplate. The above equation clearly demonstrates that the alignment signal is proportional to $(<\cos^2\theta> - 1/3)$ for pure heterodyne detection. Thus, the raw pure heterodyne signal directly reproduced the expected $\langle\cos^2\theta\rangle$ value.

Results and Discussion

1. Field-Free Alignment. The calculated revival structures of N_2, O_2, and CO irradiated by 800 nm, 110 fs laser pulses at an intensity of 2×10^{13} W/cm^2 are shown in Figures 2a, 3a, and 4a, respectively. The baseline value of $\langle\cos^2\theta\rangle$ is about 0.334, approximating an isotropic distribution of 1/3. The classical rotational period T_r of molecules is determined by the equation $T_r = 1/(2B_0c)$, where B_0 is the rotational constant of the diatomic molecule in the vibrational ground state and c is the speed of the light. For N_2, O_2, and CO, B_0 is 2.010, 1.4456, and 1.9772 cm^{-1}, respectively.[18] The corresponding rotational period T_r is therefore 8.3 ps for N_2, 11.6 ps for O_2, and 8.5 ps for CO.

The alignment signal fully revives every molecular rotational period. There are also moments of strong alignment that occur at shorter intervals. However, the three molecules exhibit different behaviors at the quarter-full revivals. The ratios of the alignment signal at quarter revivals to that at full revivals were nearly 1/3 for N_2, 1 for O_2, and 0 for CO. The large difference at the quarter-full revivals for N_2, O_2, and CO results from the different nuclear spin weights of the even and odd J states in the initial distribution. At quarter-full revivals, the odd wavepacket has maxima (minima), whereas the even wavepacket has minima (maxima). For homonuclear diatomic molecules, the nuclear spin statistics control the relative weights between even and odd J states. In the case of N_2, the relative weights of the even and odd J are 2:1. As a result, the temporary localization of the even wavepacket at quarter-full revival was partially cancelled by its odd counterpart. Thus, the alignment signal at the quarter-full revival was about 1/3 of that at the full revival for N_2. In the case of O_2, only odd J states were populated. Since only a single localized wavepacket existed, the alignment signal at the quarter-full revival was almost equal to that at the full revival for O_2. For the heteronuclear diatomic molecule CO, the opposite localizations of the even and the odd wavepackets would cancel each other. Therefore, no net alignment would be observed at the time of the quarter-full revival.

Figures 2b, 3b, and 4b display the homodyne signal versus the pump−probe delay for N_2, O_2, and CO irradiated by 800 nm, 110 fs laser pulses at an intensity of 2×10^{13} W/cm^2. The signal was proportional to $[<\cos^2\theta> - 1/3]^2$. Each peak denotes the alignment moment with the molecular axis parallel to the pump laser polarization direction ($\langle\cos^2\theta\rangle > 1/3$) or perpendicular to the pump laser polarization direction ($\langle\cos^2\theta\rangle < 1/3$). For the intervals between the alignments, the angular distribution of the molecules was isotropic relative to the laser polarization direction ($\langle\cos^2\theta\rangle = 1/3$). Although the homodyne signal clearly determined the moment that the alignment occurred, it could not indicate whether the aligned molecules were parallel or perpendicular to the laser polarization direction.

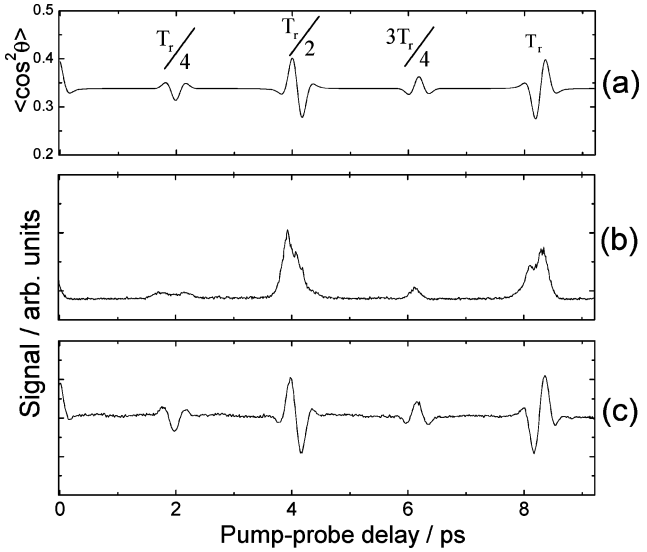

Figure 2. Revival structure of N_2 irradiated by an 800 nm, 110 fs pulse at an intensity of 2×10^{13} W/cm^2; (a) numerical calculation, (b) homodyne signal, (c) pure heterodyne signal.

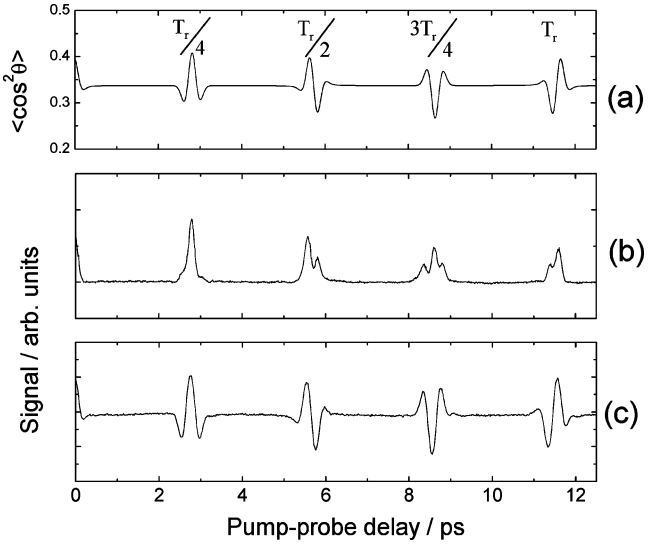

Figure 3. Revival structure of O_2 irradiated by an 800 nm, 110 fs pulse at an intensity of 2×10^{13} W/cm^2; (a) numerical calculation, (b) homodyne signal, (c) pure heterodyne signal.

Figures 2c, 3c, and 4c display the pure heterodyne signal versus the pump−probe delay for N_2, O_2, and CO irradiated by 800 nm, 110 fs laser pulses at an intensity of 2×10^{13} W/cm^2. The signal was proportional to ($<\cos^2\theta>$ − 1/3). Compared with the numerically calculated alignment parameter $<\cos^2\theta>$, there is only a baseline (∼1/3) shift. Thus, the heterodyne signal directly reproduced the revival structure of molecules under the field-free condition.

2. Fourier Transform of the Time-Dependent Alignment Signals. The Fourier transform spectrum of the time-dependent alignment parameter $\langle\cos^2\theta\rangle$ signal contains a series of beat frequencies $\Delta\omega$ between adjacent J states, which are given by

$$\Delta\omega_{J,J+2} = \frac{E_{J+2} - E_J}{\hbar} = (4J + 6)\omega_0 \qquad (12)$$

where $\omega_0 = 2\pi B_0 c$ is the fundamental phase frequency. The amplitude of the beat frequency $\Delta\omega_{J,J+2}$ is proportional to $|A_J||A_{J+2}|$, the products of the expanding coefficients. These coefficients contain information regarding the populations of the different $|J\rangle$ states in the rotational wavepacket.

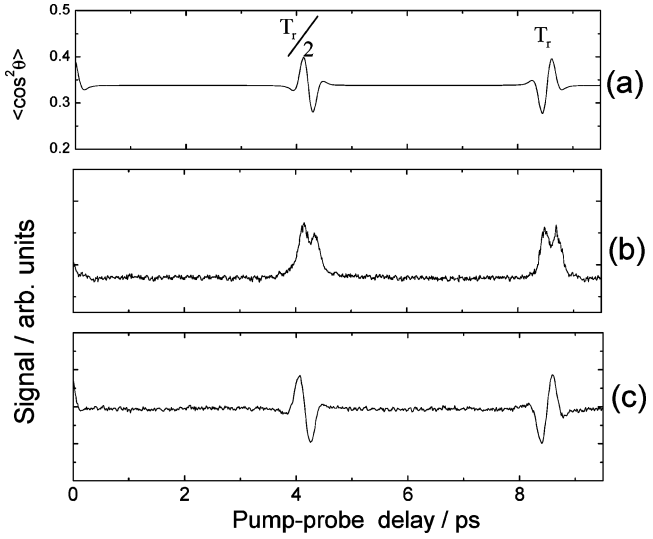

Figure 4. Revival structure of CO irradiated by an 800 nm, 110 fs pulse at an intensity of 2×10^{13} W/cm^2; (a) numerical calculation, (b) homodyne signal, (c) pure heterodyne signal.

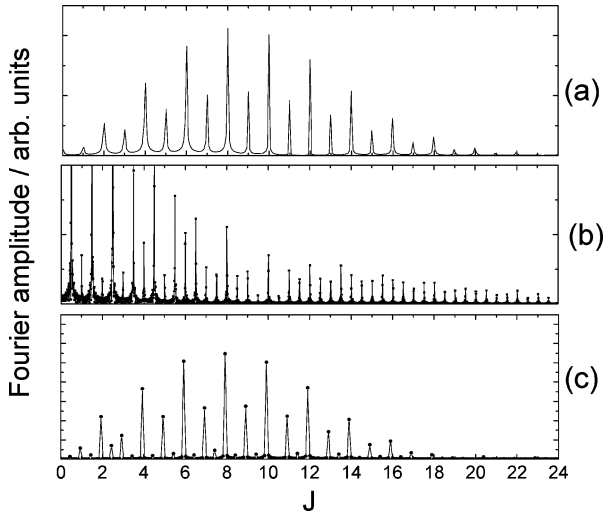

Figure 5. Fourier transforms of the revival structure of N_2 shown in Figure 2.

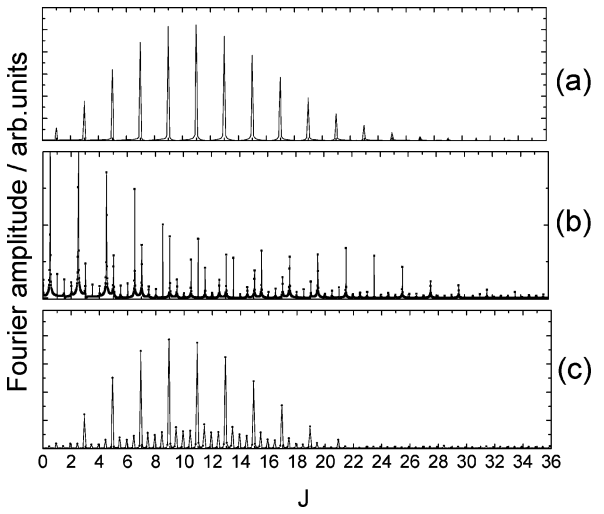

Figure 6. Fourier transforms of the revival structure of O_2 shown in Figure 3.

Figures 5a, 6a, and 7a show the Fourier transform spectra of the calculated $\langle\cos^2\theta\rangle$ in Figures 2a, 3a, and 4a. In the present study, the beat frequency $\Delta\omega$ is directly replaced by the

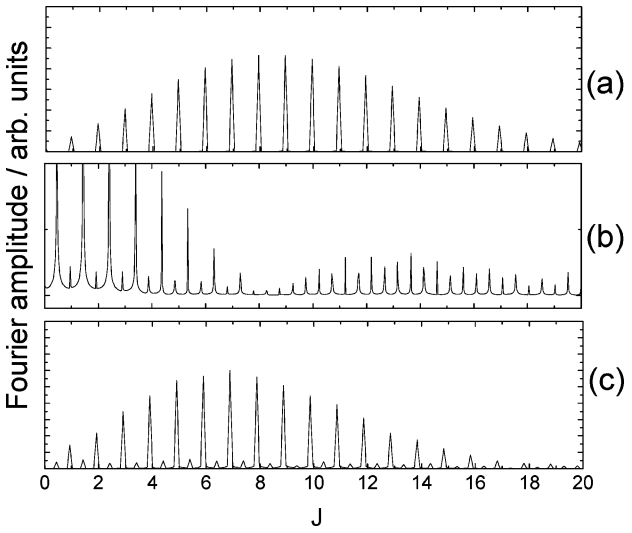

Figure 7. Fourier transforms of the revival structure of CO shown in Figure 4.

rotational quantum number *J*, and all of the Fourier transforms of the alignment signals span three full periods of the molecules. Each spectrum describes the revival structure decomposing into different $|J\rangle$ states. The nuclear spin statistics were clearly demonstrated by the amplitudes of beats between even *J* states over odd *J* states. There is a ~2:1 intensity alternation between even *J* and odd *J* states for N_2, but there are only odd *J* states for O_2. The difference of the relative weights between even and odd *J* states resulted in different alignment signals at quarter revivals for these molecules.

Figures 5b, 6b, and 7b show the Fourier transform spectra of the homodyne signals in Figures 2b, 3b, and 4b. The beat frequencies were more than the fundamental frequencies. They also included the sum and the difference frequencies. The front progression is the difference frequencies, the middle progression is the fundamental frequencies, and the end is the sum frequencies. However, the Fourier amplitudes of the fundamental frequencies were minor for the Fourier transform of the homodyne signal, even though they contained information regarding the populations of different *J* states in the rotational wavepacket.

Figures 5c, 6c, and 7c show the Fourier transform spectra of the pure heterodyne signals in Figures 2c, 3c, and 4c. In comparison with the contribution from the complicated beat frequencies in the homodyne signal, the contribution from the fundamental frequencies dominated in the Fourier transform spectrum of the pure heterodyne signal. The Fourier transform spectrum of the heterodyne signal was very similar to that of the calculated alignment parameter $<\cos^2\theta>$, which provided information regarding the populations of different *J* states in the rotational wavepacket.

3. Discussion. Field-free-aligned molecules have been the topics of rapidly growing experimental and theoretical interest in recent years. Much effort has been given to develop experimental methods to evaluate the alignment degree of molecules.[10−14,19] Currently, two typical methods have been developed. One is Coulomb explosion or dissociative ionization, in which the aligned molecules were quickly broken by another strong probe laser pulse and the angular distributions of the fragmental ions reproduced the alignment parameter $<\cos^2\theta>$. The other is a weak-field polarization technique, in which another weak probe laser pulse was used to measure the depolarization induced by the transient aligned molecules. The alignment signal is proportional to $[<\cos^2\theta> - 1/3]^2$. These two existing methods have obvious advantages and disadvantages. The former has the advantage that the alignment parameter $<\cos^2\theta>$ is directly reproduced by the angular distribution of explosion fragments and the disadvantage that the probe laser pulse is so strong that it destroys the aligned molecules. The latter has the advantage that the weak probe laser does not destroy the aligned molecules or induce extra alignment. However, it has the disadvantage that the alignment signal cannot provide the direct information of the alignment parameter $<\cos^2\theta>$. For example, the homodyne signal cannot demonstrate whether the aligned molecule is parallel or perpendicular to the laser polarization direction. The pure heterodyne detection we provided here combines the advantages of the two existing methods and avoids their disadvantages. The pure heterodyne signal directly reproduces the alignment parameter $<\cos^2\theta>$, but it does not destroy the aligned molecules.

The Fourier transform of the time-dependent alignment parameter $<\cos^2\theta>$ provides the population distribution information of *J* states which comprise the rotational wavepacket.[20] For Coulomb explosion or the dissociative ionization method, the alignment signal directly reproduced the alignment parameter $<\cos^2\theta>$; its Fourier transform spectrum only contained the contribution from the fundamental frequencies and provided information regarding the populations of different *J* states in the rotational wavepacket.[11,21] However, for the weak-field polarization technique, the alignment signal is proportional to $[<\cos^2\theta> - 1/3]^2$. Its Fourier transform spectrum contained the contribution not only from the fundament frequencies but also from the difference and sum frequencies. In addition, the contributions from the fundamental frequencies were minor even though they provided information regarding the populations of different *J* states in the rotational wavepacket. The pure heterodyne signal was proportional to $(<\cos^2\theta> - 1/3)$. The Fourier transform spectrum of the pure heterodyne signal was very similar to that of the calculated alignment parameter $<\cos^2\theta>$, which provided information regarding the populations of different *J* states in the rotational wavepacket.

Conclusions

We modified the typical weak-field polarization technique. The homodyne detection and the heterodyne detection were realized in an apparatus. They were utilized to quantify the field-free alignments of diatomic molecules N_2, O_2, and CO irradiated by strong femtosecond laser pulses. The alignment signal was proportional to $[<\cos^2\theta> - 1/3]^2$ for homodyne detection and $(<\cos^2\theta> - 1/3)$ for pure heterodyne detection. Fourier transform spectra of the homodyne signal and the pure heterodyne signal were also studied. Compared with the existing detection methods, the pure heterodyne detection had the following advantages. First, the pure heterodyne signal directly reproduced the alignment parameter $<\cos^2\theta>$ without destroying the aligned molecules. Second, the Fourier transform spectrum of the pure heterodyne signal was very similar to that of the calculated alignment parameter $<\cos^2\theta>$ and provided information regarding the populations of different *J* states in the rotational wavepacket.

Acknowledgment. This work was supported by the National Natural Science Foundation of China under Grant Nos. 20603001, 10534010, 10634020, and 10521002 and the National Basic Research Program of China under Grant No. 2006CB806007.

References and Notes

(1) Friedrich, B.; Herschbach, D. *Phys. Rev. Lett.* **1995**, *74*, 4623.
(2) Seideman, T. *J. Chem. Phys.* **1995**, *103*, 7887.

(3) Stapelfeldt, H.; Seideman, T. *Rev. Mod. Phys.* **2003**, *75*, 543.
(4) Seideman, T. *Phys. Rev. Lett.* **1999**, *83*, 4971.
(5) Ortigoso, J.; Rodríguez, M.; Gupta, M.; Friedrich, B. *J. Chem. Phys.* **1999**, *110*, 3870.
(6) Seideman, T. *J. Chem. Phys.* **2001**, *115*, 5965.
(7) Litvinyuk, L. V.; Lee, K. F.; Dooley, P. W.; Rayner, D. M.; Villeneuve, D. M.; Corkum, P. B. *Phys. Rev. Lett.* **2003**, *90*, 233003.
(8) Itatani, J.; Levesque, J.; Zeidler, D.; Niikura, H.; Pepin, H.; Kieffer, J. C.; Corkum, P. B.; Villeneuve, D. M. *Nature* **2004**, *432*, 7019.
(9) Kanai, T.; Minemoto, S.; Sakai, H. *Nature* **2005**, *435*, 470.
(10) Rosca-Pruna, F.; Vrakking, M. J. J. *Phys. Rev. Lett.* **2001**, *87*, 153902.
(11) Dooley, P. W.; Litvinyuk, I. V.; Lee, K. F.; Rayner, D. M.; Spanner, M.; Villeneuve, D. M.; Corkum, P. B. *Phys. Rev. A* **2003**, *68*, 023406.
(12) Renard, V.; Renard, M.; Guerin, S.; Pashayan, Y. T.; Lavorel, B.; Faucher, O.; Jauslin, H. R. *Phys. Rev. Lett.* **2003**, *90*, 153601.
(13) Renard, V.; Renard, M.; Rouzee, A.; Guerin, S.; Jauslin, H. R.; Lavorel, B.; Faucher, O. *Phys. Rev. A* **2004**, *70*, 033420.
(14) Renard, V.; Faucher, O.; Lavorel, B. *Opt. Lett.* **2005**, *30*, 70.
(15) Xu, N.; Wu, C.; Huang, J.; Wu, Z.; Liang, Q.; Yang, H.; Gong, Q. *Opt. Express* **2006**, *14*, 4992.
(16) Press W. H.; Teukolsky, S. A.; Vetterling, W. T.; Flannery, B. P. *Numerical Recipes*, 2nd ed.; Cambridge University Press: Cambridge, England, 1992.
(17) Levenson, M. D. *Introduction to Nonlinear Laser Spectroscopy*; Academic Press: New York, 1982.
(18) Herzberg, G. *Molecular Spectra and Molecular Structure*; Van Nostrand Reinhold Company Ltd.: New York, 1966.
(19) Zamith, S.; Ansari, Z.; Lepine, F.; Vrakking, M. J. J. *Opt. Lett.* **2005**, *30*, 2326.
(20) Seideman, T.; Hamilton, E. *Adv. At. Mol. Opt. Phys.* **2005**, *52*, 289.
(21) Bryan, W. A; English E. M. L.; McKenna J.; Wood, J.; Calvert, C. R.; Turcu, I. C. E.; Torres, R.; Collier, J. L.; Williams, I. D.; Newell, W. R. *Phys. Rev. A* **2007**, *76*, 023414.